# Possible NMSSM Benchmark Points for Run II

Conny Beskidt, Wim de Boer, Dmitri Kazakov, Stefan Wayand
Karlsruhe Institute of Technology, IEKP

**Abstract**

In the MSSM the heaviest scalar and pseudoscalar boson decay into b-quarks and tau-leptons in the large $\tan\beta$ scenario, preferred by the relic density constraint. In the NMSSM such decays are absent and the decay of the heavy Higgs bosons is preferentially into top quark pairs (if kinematiccally allowed) or lighter Higgs bosons and the LSPs, leading to invisible decays. We propose two benchmark points, which represesnt these salient NMSSM features.

## 1 Introduction

The additional Higgs singlet in the NMSSM and its corresponding supersymmetric partner, the singlino, modify the Higgs phenomenology drastically, as can be seen most clearly from the branching ratios of the heavy scalar Higgs boson: in the MSSM the heavy Higgs boson H decays predominantly into b-quarks and tau leptons, while in the NMSSM these decay modes are typically absent and the decays into top quarks (when above threshold) or lighter Higgs bosons prevail. The large difference in the BR between the NMSSM and MSSM is demonstrated in Figs. 1 and 2. Since the heavy pseudoscalar and heavy scalar Higgs bosons have almost equal masses, it is important to consider them simultaneously. In the MSSM they have similar branching ratios, but in the NMSSM they can differ, if the mass is below the $t\bar{t}$ threshold, as can be seen from a comparison of Figs. 1 and 3.

The suppression of the ttbar decay mode of the heavy Higgs boson in the MSSM is given by the relatively large values of $\tan\beta$, required by the relic density constraint. In the NMSSM the relic density is usually always fulfilled, because of the many more parameters and the many more annihilation channels in the enriched Higgs sector. Furthermore, the requirement of $M_{H2} = 125$ GeV leads to small $\tan\beta$ (between 2 and 5) in the NMSSM, so the $B_s \to \mu\mu$ decay modes (proportional to $\tan^6\beta$) are not constraining. Actually, the only constraints on the NMSSM parameter space are the LHC searches, although in combination with the relic density small values for the lightest Higgs boson masses are excluded.

For heavier Higgs masses, the branching ratios for charginos and neutralinos increase as well, if they are not too heavy, as shown in Fig. 1. The gaugino

Table 1: Masses of the Higgs bosons for BMP1 (large $t\bar{t}$ BR ) and BMP2 ($H_1H_2$ decay dominant) and the corresponding Higgs production cross section at 14 TeV for the dominant gluon-gluon fusion process.

| mass in GeV | BMP1 | BMP2 | $\sigma_{prod}$ in pb (BMP1) | $\sigma_{prod}$ in pb (BMP2) |
|---|---|---|---|---|
| $H_1$ | 90.00 | 90.00 | 1.114 | 1.371 |
| $H_2$ | 125.47 | 125.15 | 49.554 | 49.417 |
| $H_3$ | 450.00 | 349.01 | 1.817 | 3.332 |
| $A_1$ | 300.00 | 300.00 | 0.144 | 0.185 |
| $A_2$ | 446.27 | 342.14 | 3.963 | 12.356 |

masses were chosen to correspond to a CMSSM mass point not excluded by the LHC ($m_0$=1000, $m_{1/2}$=850 GeV). Note that the Higgs masses are largely independent of the SUSY masses. The bands in Fig. 1 were obtained in the following way. A certain set of NMSSM parameters produces a certain set of Higgs masses. Alternatively, one can invert the problem and consider the paramater space to be the masses of the 5 neutral Higgs bosons, which is easier to interpret than the NMSSM parameters. Given the masses one can use Minuit to determine the corresponding NMSSM parameters, either at the GUT scale or at the electroweak scale. We have chosen to take the parameters at the GUT scale, since then the complete radiative corrections from the GUT scale to the electroweak scale are taken into account in the spectrum calculators. We used NMSSM Tools 4.6.0 to calculate the spectrum. In the Minuit fit we added the following constraints: $H_2 = 125$ GeV with couplings agreeing within 10% with the SM couplings, the LSP (largely singlino) provides the relic density and gives a nucleon scattering cross section consisten with the direct DM searches. These dark matter constraints are calculated with micrOmegas within NMSSMTools. By scanning over the 5 neutral Higgs boson masses with the above constraints yielded the bands in Fig. 1.

We propose two benchmark points: one in which the heavy scalar Higgs decays mostly into $t\bar{t}$ BR ) (called BMP1) and one, in which the heavy scalar Higgs decays decays mostly into $H_1H_2$ (called BMP2). Since the heavy pseudoscalar Higgs mass is almost degenerate in mass with the scalar one, they will be produced simultaneously, but with different branching ratios and cross sections. The masses and cross sections have been summarized in Table 1. In the following we discuss some of the features of these benchmark points. The NMSSMTools input and output files for these two benchmark points have been attached (filename with h1h2 for BMP2 and tt for BMP1).

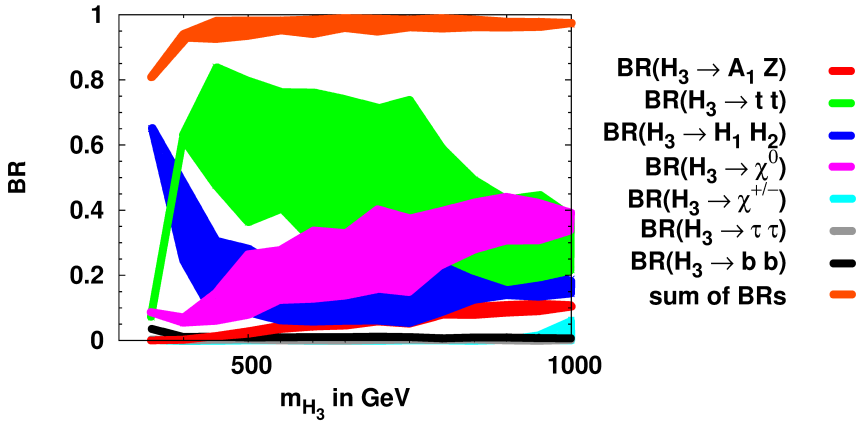


Figure 1: The branching ratios of the heavy Higgs boson $H_3$ in the NMSSM as function of its mass. There are negligible decays into gauge boson pairs, $b\bar{b}$ and $\tau\bar{\tau}$. Decays into gaugino masses become possible as well, if they are light enough. Here they were chosen to correspond to a CMSSM mass point not excluded by the LHC ($m_0$=1000, $m_{1/2}$=850 GeV).

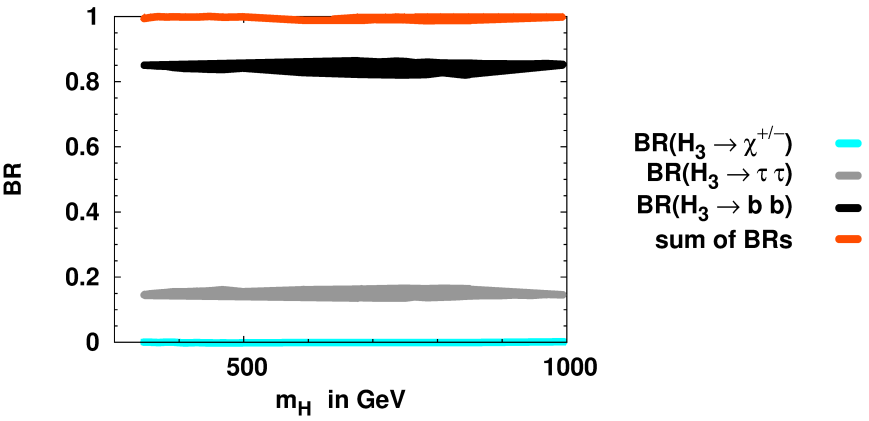


Figure 2: As in Fig. 1, but for the heavy Higgs boson $H$ in the MSSM. There are no decays into gauge bosons and the decay into $t\bar{t}$ is suppressed by the large value of $\tan\beta$, required by the relic density in most of the parameter space.

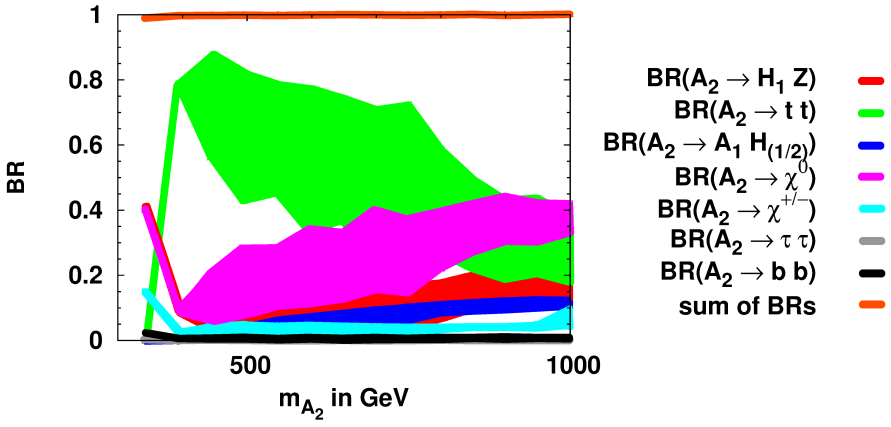


Figure 3: As in Fig. 1, but for the pseudoscalar Higgs boson $A_2$ in the NMSSM as function of its mass. Below the top threshold the decay is predominantly into $Z + H_1$ instead of $H_1 + H_2$ for the $H_2$ scalar boson. The latter always has a mass close to the $A_2$ mass, but usually a smaller production cross section (see Table 1). If the LSPs are light enough, they contribute significantly below the ttbar threshold.

Table 2: Summary of the dominant BRs of heavy Higgs bosons for BMP1(large $t\bar{t}$ BR ), which has $m_{H_1} = 90$, $m_{H_2} = 125$, $m_{H_3} = 450$,$m_{A_2} = 446$, $m_{A_1} = 300$, LSP=151 GeV. GeV. The cross section represents the Higgs production at 14 TeV for the dominant gluon-gluon fusion process.

| | |
|---|---|
| $H_3 \to H_1 H_2$ | 22.4 |
| $H_3 \to t\bar{t}$ | 56.6 |
| $H_3 \to H_1 H_1$ | 2.5 |
| $H_3 \to A_1 Z$ | 1.5 |
| $H_3 \to \chi_1^0 \chi_1^0$ | 8.9 |
| $H_3 \to \chi_1^0 \chi_2^0$ | 1.0 |
| $H_3 \to \chi_1^0 \chi_3^0$ | 3.9 |
| $H_3 \to \chi_1^+ \chi_1^-$ | 1.6 |
| $\sigma_{prod}$ in pb | 1.82 |
| $A_2 \to A_1 H_2$ | 1.4 |
| $A_2 \to t\bar{t}$ | 66.2 |
| $A_2 \to A_1 H_1$ | 1.3 |
| $A_2 \to H_1 Z$ | 11.3 |
| $A_2 \to \chi_1^0 \chi_1^0$ | 13.1 |
| $A_2 \to \chi_1^0 \chi_2^0$ | 0.8 |
| $A_2 \to \chi_1^0 \chi_3^0$ | 0.9 |
| $A_2 \to \chi_1^+ \chi_1^-$ | 4.2 |
| $\sigma_{prod}$ in pb | 3.99 |

# 2 Benchmark Point BMP1 with $t\bar{t}$ decay dominant

The branching ratios of the heavy Higgs bosons $H_2$ and $A_2$ are shown in Table 2. Both bosons have practically the same mass (450 and 446GeV, respectively). In both cases the $t\bar{t}$ decay is dominant (see Table 2, so the cross sections can be added (around 6 pb in total). Note that $H_3$ can decay into $H_1+H_2$ as well, while for $A_2$ the decay into $H_1 + Z$ yields the second largest BR. $A_1$ decays largely into $Z + H_1$, as shown in Table 3. So this benchmark point is characterized by a large fraction of ttbar final states, which can be searched for as a broad bump around 450 GeV in the tail of the ttbar invariant mass spectrum. Furthermore, events with two Z bosons and the $H_1$ Higgs boson of 90 GeV with practically SM decay modes can be searched for from the $A_2$ decay mentioned above.

Table 3: Branching ratios of the lighter Higgs bosons in BMP1 ($t\bar{t}$ dominant).

| | |
|---|---|
| $H_1 \to b\bar{b}$ | 90.2 |
| $H_1 \to \tau\tau$ | 9.4 |
| $H_2 \to b\bar{b}$ | 61.4 |
| $H_2 \to WW$ | 20.6 |
| $H_2 \to gg$ | 5.7 |
| $H_2 \to \tau\tau$ | 6.7 |
| $H_2 \to c\bar{c}$ | 2.8 |
| $H_2 \to ZZ$ | 2.3 |
| $A_1 \to gg$ | 1.4 |
| $A_1 \to \tau\tau$ | 1.7 |
| $A_1 \to b\bar{b}$ | 12.9 |
| $A_1 \to ZH_1$ | 83.4 |
| $A_1 \to \chi_1^0\chi_1^0$ | - |

# 3 Benchmark Point BMP2 with $H_1H_2$ decay dominant

The branching ratios of the heavy Higgs bosons $H_2$ and $A_2$ are shown in Table 4. Both bosons have practically the same mass (349 and 342 GeV, respectively), ut they have quite different decays in contrast to BMP1: $H_3$ decays for 64% into $H_1 + H_2$, while $A_2$ decays for 39% into $H_1 + Z$ and the remaining decay modes are largely gauginos. The decay mode of $A_1$ is not $Z + H_1$ anymore, as in BMP1 (although the masses of the lighter Higgs bosons are identical), but the main decay mode is now into LSPs, so an invisible final state. as shown in Table 5. So this benchmark point is characterized by a large fraction of double Higgs prodution in the $H_2$ decay, while the $A_2$ decays into $Z + H_1$ or gauginos, either neutral or charged, which in turn have a rich spectrum of decay modes (see Table 6). The $A_1$ boson decays largely into invisible neutralinos, while the lightest Higgs boson $H_1$ decays largely into $b\bar{b}$ and tau-pairs.

Table 4: Summary of heavy Higgs boson branching ratios (in %) in BMP2, which has $m_{H_1} = 90$, $m_{H_2} = 125$, $m_{H_3} = 349$, $m_{A_2} = 342$, $m_{A_1} = 300$, LSP=131 GeV. The cross sections represent the Higgs production at 14 TeV for the dominant gluon-gluon fusion process.

| | |
|---|---|
| $H_3 \to H_1 H_2$ | 63.9 |
| $H_3 \to t\bar{t}$ | 7.5 |
| $H_3 \to H_1 H_1$ | 9.3 |
| $H_3 \to A_1 Z$ | - |
| $H_3 \to \chi_1^0 \chi_1^0$ | 8.6 |
| $H_3 \to \chi_1^0 \chi_2^0$ | 0.3 |
| $H_3 \to \chi_1^0 \chi_3^0$ | - |
| $H_3 \to \chi_1^+ \chi_1^-$ | 4.7 |
| $\sigma_{prod}$ in pb | 3.33 |
| $A_2 \to A_1 H_2$ | - |
| $A_2 \to t\bar{t}$ | - |
| $A_2 \to A_1 H_1$ | - |
| $A_2 \to H_1 Z$ | 39.2 |
| $A_2 \to \chi_1^0 \chi_1^0$ | 41.3 |
| $A_2 \to \chi_1^0 \chi_2^0$ | 0.2 |
| $A_2 \to \chi_1^0 \chi_3^0$ | - |
| $A_2 \to \chi_1^+ \chi_1^-$ | 15.7 |
| $\sigma_{prod}$ in pb | 12.36 |

Table 5: Branching ratios (in %) of the lighter Higgs bosons in BMP2 ( $H_1 H_2$ dominant).

| | |
|---|---|
| $H_1 \to b\bar{b}$ | 90.1 |
| $H_1 \to \tau\tau$ | 9.4 |
| $H_2 \to b\bar{b}$ | 62.1 |
| $H_2 \to WW$ | 19.9 |
| $H_2 \to gg$ | 5.7 |
| $H_2 \to \tau\tau$ | 6.8 |
| $H_2 \to c\bar{c}$ | 2.8 |
| $H_2 \to ZZ$ | 2.2 |
| $A_1 \to gg$ | 0.0 |
| $A_1 \to \tau\tau$ | 0.0 |
| $A_1 \to b\bar{b}$ | 0.0 |
| $A_1 \to Z H_1$ | 1.1 |
| $A_1 \to \chi_1^0 \chi_1^0$ | 98.7 |

Table 6: Typical neutralino and chargino decays with branching ratios in % (BMP2).

| | |
|---|---|
| $\chi_1^+ \to \chi_1^0 u\bar{d}$ | 33.4 |
| $\chi_1^+ \to \chi_1^0 c\bar{c}$ | 33.4 |
| $\chi_1^+ \to \chi_1^0 e^+ \nu_e$ | 11.2 |
| $\chi_1^+ \to \chi_1^0 \mu^+ \nu_\mu$ | 11.2 |
| $\chi_1^+ \to \chi_1^0 \tau^+ \nu_\tau$ | 10.8 |
| $\chi_2^0 \to \chi_1^0 \bar{u} u$ | 8.8 |
| $\chi_2^0 \to \chi_1^0 \bar{d} d$ | 11.4 |
| $\chi_2^0 \to \chi_1^0 \bar{c} c$ | 8.8 |
| $\chi_2^0 \to \chi_1^0 \bar{s} s$ | 11.4 |
| $\chi_2^0 \to \chi_1^0 \bar{b} b$ | 10.9 |
| $\chi_2^0 \to \chi_1^0 e^+ e^-$ | 2.6 |
| $\chi_2^0 \to \chi_1^0 \mu^+ \mu^-$ | 2.6 |
| $\chi_2^0 \to \chi_1^0 \tau^+ \tau^-$ | 2.6 |
| $\chi_2^0 \to \chi_1^0 \bar{\nu}_e \nu_e$ | 5.2 |
| $\chi_2^0 \to \chi_1^0 \bar{\nu}_\mu \nu_\mu$ | 5.2 |
| $\chi_2^0 \to \chi_1^0 \bar{\nu}_\tau \nu_\tau$ | 5.2 |
| $\chi_2^0 \to \chi_1^+ \bar{u} d$ | 4.2 |
| $\chi_2^0 \to \chi_1^+ \bar{d} u$ | 4.2 |
| $\chi_2^0 \to \chi_1^+ \bar{c} s$ | 4.2 |
| $\chi_2^0 \to \chi_1^+ \bar{s} c$ | 4.2 |
| $\chi_2^0 \to \chi_1^+ \bar{\nu}_e e^-$ | 1.4 |
| $\chi_2^0 \to \chi_1^+ \nu_e e^+$ | 1.4 |
| $\chi_2^0 \to \chi_1^+ \bar{\nu}_\mu \mu^-$ | 1.4 |
| $\chi_2^0 \to \chi_1^+ \nu_\mu \mu^+$ | 1.4 |
| $\chi_2^0 \to \chi_1^+ \bar{\nu}_\tau \tau^-$ | 1.4 |
| $\chi_2^0 \to \chi_1^+ \nu_\tau \tau^+$ | 1.4 |
| $\chi_3^0 \to \chi_1^0 Z$ | 60.2 |
| $\chi_3^0 \to \chi_1^0 H_1$ | 31.2 |
| $\chi_3^0 \to \chi_1^+ \bar{u} d$ | 1.4 |
| $\chi_3^0 \to \chi_1^- \bar{d} u$ | 1.4 |
| $\chi_3^0 \to \chi_1^+ \bar{c} s$ | 1.4 |
| $\chi_3^0 \to \chi_1^- \bar{s} c$ | 1.4 |
| $\chi_4^0 \to \chi_1^0 Z$ | 1.7 |
| $\chi_4^0 \to \chi_2^0 Z$ | 12.8 |
| $\chi_4^0 \to \chi_1^+ W^-$ | 29.5 |
| $\chi_4^0 \to \chi_1^- W^+$ | 29.5 |
| $\chi_4^0 \to \chi_1^0 H_1$ | 7.7 |
| $\chi_4^0 \to \chi_1^0 H_2$ | 14.7 |
| $\chi_4^0 \to \chi_3^0 H_1$ | 1.5 |
| $\chi_4^0 \to \chi_3^0 H_2$ | 1.6 |
| $\chi_5^0 \to \chi_1^0 Z$ | 2.0 |
| $\chi_5^0 \to \chi_2^0 Z$ | 17.7 |
| $\chi_5^0 \to \chi_1^+ W^-$ | 20.6 |
| $\chi_5^0 \to \chi_1^- W^+$ | 20.6 |
| $\chi_5^0 \to \chi_1^0 H_1$ | 1.6 |
| $\chi_5^0 \to \chi_1^0 H_2$ | 14.5 |
| $\chi_5^0 \to \chi_1^0 A_2$ | 2.5 |
| $\chi_5^0 \to \chi_2^0 H_3$ | 2.4 |
| $\chi_5^0 \to \chi_2^0 A_2$ | 1.0 |
| $\chi_5^0 \to \chi_3^0 H_2$ | 1.8 |
| $\chi_5^0 \to \chi_4^0 H_2$ | 1.6 |
| $\chi_5^0 \to \chi_1^+ H^-$ | 5.0 |
| $\chi_5^0 \to \chi_1^- H^+$ | 5.0 |